

Cotunneling current affected by spin-polarized wire molecules in networked gold nanoparticles

Tadashi Sugawara,^{*} Masaru Minamoto, Michio M. Matsushita, Patrick Nickels, and Susumu Komiyama[†]
*Department of Basic Science, Graduate School of Arts and Sciences, The University of Tokyo, Komaba,
 Meguro-ku, Tokyo 153-8902, Japan*

(Received 15 March 2008; revised manuscript received 22 May 2008; published 20 June 2008)

As a bottom-up approach toward spintronics, a network structure of gold nanoparticles connected with spin-polarized wire molecules has been studied. A spinless network is prepared as a reference system. The network of gold nanoparticles with an average diameter of 4 nm form granules (average diameter of 100 nm), which in turn, connect themselves with each other to bridge 2 μm -gap gold electrodes. Since the charging energy of a 4-nm gold nanoparticle amounts to 160 meV, it works as a Coulomb island and the conduction through the network is dominated by Coulomb blockade effect at room temperature. Thermal-activation-type conduction is found in a temperature range of 300 K–30 K, below which cotunneling is suggested to dominate. Important findings reported here are as follows: (1) The cotunneling occurs at elevated temperatures as high as $T=30$ K due to the small size of gold nanoparticles: Nonlinear characteristics featured by $I\text{-}V^3$ are found, suggesting that the number of tunnel junctions relevant to the cotunneling is two. (2) The cotunneling current is substantially smaller in spin-polarized network than in spinless network, suggesting that spin-flip scattering caused by localized spins on wire molecules suppresses cotunneling process: The interpretation is supported by negative magnetoresistance observed in spin-polarized networks.

DOI: 10.1103/PhysRevB.77.235316

PACS number(s): 73.23.Hk, 75.47.Pq, 72.25.Mk, 73.63.Kv

I. INTRODUCTION

Spin-electronic devices have drawn much attention as advanced electronic devices that manipulate not only an electronic charge but also an electronic spin.^{1,2} Recently, excellent demonstrations of prototypes of spin-electronics³ have been proposed. Although a variety of methods for manipulating a spin-polarized current are conceivable, spin-electronic devices that have been so far developed either rely on a spin-polarized current emitted from ferromagnetic metal electrodes or exploit the electronic spin state realized in a quantum dot.^{4,5} Whereas endeavors to minimize the scale of silicon-based electronics have led to the concept of a molecule-based electronic device as molecular switches, transistors, and rectifiers,⁶ exploitation of molecule-based spins has scarcely been explored. As an ultimate molecule-based component for spin-electronics, we have developed spin-polarized donor molecules in which an electron donor unit is connected with a π -radical unit in a cross-conjugating manner.⁷⁻⁹ Recently we reported that the 2:1 ion-radical salt of a spin-polarized donor with perchlorate as a counter ion exhibited negative magnetoresistance without any magnetic metal ions.¹⁰

Meanwhile, a preparative method of gold nanoparticles through reduction of aurate ions (HAuCl_4) in the presence of surfactants¹¹ has been established. On the basis of these achievements, Coulomb blockade effects of isolated gold nanoparticles were experimentally demonstrated and studied in detail through scanning tunnel microscopy (STM) measurements.¹² The electronic transport properties of films of gold nanoparticles coated by alkanethiol have drawn much attention from the viewpoint of single electron tunneling. The electronic structure of a gold nanoparticle with a diameter ($2r$) of 4 nm is known to be metallic.¹³ The capacitance of a nanoparticle, $C=4\pi\epsilon_0\epsilon_r r$ with $r=2$ nm, is small, and the charging energy, $E_c=e^2/C$, amounts to ca. 80 meV in

typical organic media ($\epsilon_r=4$) according to a concentric capacitor model. Since $E_c=80$ meV largely exceeds the thermal energy (26 meV) at room temperature, the nanoparticle can work as a Coulomb island exhibiting single electron tunneling effect at room temperature. Wire molecules serve as an appropriate tunnel junction for nanoparticles with a tunnel resistance well beyond the resistance quantum, $h/e^2 \approx 26$ k Ω .

In fact, thermal-activation-type conductance, $G \propto \exp(-E_A/k_B T)$, in a temperature range of 160–100 K has been reported in multilayers of gold nanoparticles (average diameter of 5.5 nm) coated with dodecanethiol. This has been interpreted in terms of the Coulomb blockade effects of nanoparticles.¹⁴ At lower temperatures (150–25 K), the temperature dependence is described by Efros-Shklovski-type variable range hopping (ES-VRH),¹⁵ $G \propto \exp\{-(T_0/T)^{1/2}\}$, which has been interpreted on the basis of cotunneling picture.¹⁴ The T -dependence of $G \propto \exp\{-(T_0/T)^{1/2}\}$ is reported also in a wide temperature range (300–4 K) in self-assembled films of 1,4-butanedithiol linked nanoparticles with an average diameter of 4.8 ± 1.2 nm (Ref. 16). Magnetoresistance measurements suggested the occurrence of weak Anderson localization at cryogenic temperatures due to inhomogeneity in the gold nanoparticle thin films.¹⁶

In order to increase the electronic coupling between nanoparticles, networks of nanoparticles connected by π -conjugated wire molecules, such as oligothiophene-type wire molecules, have also been prepared.^{17,18} Ogawa *et al.* found threshold behavior in the I - V characteristics of networked nanoparticles at 4.2 K and discussed its relevance to the Coulomb blockade effect.¹⁷

Here, we report systematic studies of the transport property of π -bonded network of nanoparticles in a wide temperature range of 300–4 K. A molecular wire connecting gold nanoparticles serves as a well-defined tunnel barrier for the nanoparticles. We have synthesized oligothiophene-type spin-polarized wire molecules (SPM) bearing protected thiol

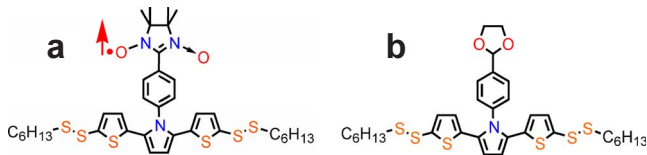


FIG. 1. (Color online) (a) Molecular structure of SPM. (b) Molecular structure of SLM.

groups at both terminals [SPM, Fig. 1(a)] for constructing networked gold nanoparticles.¹⁹ A localized spin ($s=1/2$) on the spin-polarized wire molecule is expected to serve as a spin-flip scatterer embedded in the tunnel junction. In both networks, formed by the spin-polarized and the spinless molecules [spinless wire molecule (SLM), Fig. 1(b)], we find thermal-activation-type conductance down to 50 K, below which T -dependence becomes substantially weaker. In the spinless network, the T -dependence at lower temperatures is well reproduced by theoretical predictions of cotunneling,²⁰ but is not well described by the ES-VRH relation.¹⁵ This is ascribed to the hierarchical structure of the network system in the present experiments. In the spin-polarized network, the conductance at lower temperatures (<50 K) is found to be substantially smaller than the one of the spinless network. This is interpreted as a consequence of the suppression of cotunneling due to spin-flip scattering, which is supported by the observation of negative magnetoresistance.

II. EXPERIMENT

Syntheses of SPM and SLM have been reported elsewhere.¹⁹ Interdigitated gold electrode with a gap of $2\ \mu\text{m}$ was prepared on an n -doped Si substrate covered with a $700\ \text{nm}$ -thick SiO_2 layer. The interdigitated electrodes (IDE) consist of 250 pairs of 2-mm -long parallel teeth, corresponding to an electrode with a gap of $2\ \mu\text{m}$ and a total length of $1000\ \text{mm}$. An aliquot of a toluene solution of the protected dithiol ($0.31\ \text{mM}$) was dropped on the electrodes, and after 30 min one droplet of a toluene solution of tetraoctylammonium bromide (TOAB)-stabilized 4-nm gold nanoparticles¹¹ ($11.25\ \text{mM}$) was added; the mixture was left standing for 1 h. Networks then formed as precipitates on the electrode, and they were washed with toluene and ethanol sequentially.

The structure of the resulting network of gold nanoparticles was examined by means of field-emission scanning electron microscopy (FE-SEM, JEOL JES-6700F with a working distance of $8\ \text{mm}$ and an acceleration voltage of $15.0\ \text{kV}$). An example with SPMs is shown in Fig. 2(a). For the inspection of nanostructure, transmission electron microscopy (TEM, JEOL JEM-2010 ARP with an acceleration voltage of $200\ \text{kV}$) was applied. Specimens for the TEM measurement were prepared on a copper-grid (mesh) by drying a droplet that was pipetted from a suspension obtained by mixing $1\ \text{ml}$ of a toluene solution of the SPM ($0.31\ \text{mM}$) and $1\ \text{ml}$ of a toluene solution of TOAB-stabilized nanoparticles ($11.25\ \text{mM}$).

A 4-nm (average) gold nanoparticle is composed of ca. 1750 gold atoms.¹³ Elemental analysis of the network with

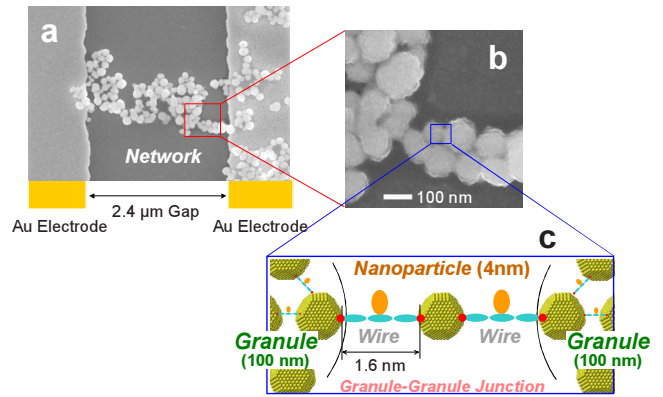


FIG. 2. (Color online) SEM image of networked gold nanoparticles with SPMs on the interdigitated electrodes with a gap of $2\ \mu\text{m}$ (a) Expanded image of a bottle-necked structure at granule-granule junction (b) Expanded picture of a granule-granule junction consisting of a granule (ca. $100\ \text{nm}$), a wire molecule, a nanoparticle, a wire molecule, and a granule, in series (c).

SPM wires showed that C:H:N:ash= $4.38\%:0.64\%:0.28\%:91.3\%$, indicating that the ratio of @Au1750/SPM wire molecule/hexanethiol/TOAB is $1:17:17:22$. Because the molecular wire is shared by two nanoparticles, this ratio means that 34 molecules of wires and hexanethiol and 22 molecules of TOAB are absorbed on a gold nanoparticle. Magnetic susceptibilities of the SPM and SLM networks were measured by a superconducting quantum interference device (SQUID) magnetometer (Quantum Design MPMS-5XL). The χT versus temperature plot of the SPM network indicates that paramagnetic spins of the wire molecules exhibit a small antiferromagnetic interaction with $\theta=0.18\ \text{K}$. The Curie constant ($C=5.55\ \text{emu K mol}^{-1}$) evaluated from the intercept suggests that about 15 spins are on a nanoparticle on average.¹⁹ The SLM network contains a tiny amount of impurity spin; less than one spin per one gold nanoparticle containing ca. 1750 gold atoms.²¹

Conductance measurements were carried out by using a Keithley 6487 picoammeter with a constant bias voltage of $0.1\ \text{V}$. The sample was placed in a temperature controlled cryostat (Quantum Design MPMS-5XL; $4\ \text{K}$ – $300\ \text{K}$). Current-voltage characteristics were studied with a source meter (Keithley 6430) via a step-sweep- or a pulse-method. Magnetoresistance measurements were made by $6\ \text{T}$ using a superconducting solenoid ($6\ \text{T}$) in a liquid helium cryostat, where the current was recorded with a picoammeter (Keithley 6487) with bias voltage of $1\ \text{V}$.

III. RESULTS AND DISCUSSION

A. Formation of the network structure

A network structure was constructed by connecting 4-nm gold nanoparticles¹¹ with SPM or SLM of a length of ca. $1.6\ \text{nm}$. Our SPM (Ref. 19) consists of three parts: a spin-polarizing core made of a pyrrole-based donor radical, a molecular wire made of a thiophene-pyrrole-thiophene hybrid trimer, and connecting parts consisting of heterodisulfide groups at terminals. Our SLM was also prepared as a reference compound.

Taking into account the band gap ($\Delta E_g=3.52$ eV), the ionization potential ($I_p=7.43$ eV) of terthiophene,^{22,23} and the work function of gold ($W=5.4$ eV),²⁴ we expect that the Fermi level of 4 nm-diameter gold nanoparticles is located between the energy levels of the highest occupied molecular orbital (HOMO) and lowest unoccupied molecular orbital (LUMO) of the wire molecule. Because the relevant energy levels are not far away from the Fermi level, it is probable that the wave function of conduction electrons in gold nanoparticles slightly penetrates into wire molecules, being hybridized with molecular orbitals.²⁵ Since the unpaired electron in SPM is localized at the nitronyl nitroxide group and the energy level of the singly occupied molecular orbital (SOMO) is lower than the delocalized HOMO along the wire part, the unpaired electron does not participate in the electron tunneling directly. However, SOMO and HOMO interact with each other through nearby occupied orbitals, which have probability amplitudes spreading over the entire molecule. Thus HOMO, which mainly contributes to the electron tunneling, can be spin-polarized by the SOMO. Under such circumstance it is highly likely that an electron tunneling between adjacent gold nanoparticles is exchange-coupled with the unpaired electron in the SOMO of the spin-polarized wire molecule.

Networked gold nanoparticles were prepared on an IDE with a gap of 2 μm by mixing solutions of SPMs or SLMs with a length of 1.6 nm and surfactant-stabilized 4 ± 0.5 nm gold nanoparticles. An FE-SEM image [Fig. 2(a)] shows that the network is of a hierarchical structure; viz., granules with a diameter of approximately 100 nm are formed, and the granules are connected to form a chain bridging the electrodes.²⁶ The network structure constructed by SLM is almost the same as the SPM network. Each granule is expected to consist of ca. 5,800 gold nanoparticles. Though not shown here, we have confirmed through TEM images that the gold nanoparticles in each granule are separated from one another by a gap of 1.6 nm, which corresponds to the length of wire molecules.¹⁹ A series of more than 20 granules is necessary for bridging the 2 μm -gap electrode. The inspection of the FE-SEM image suggests that an average number of granule-granule junctions, N_j , is 30 in one bridge. As shown by an expanded image [Fig. 2(b)], only a few nanoparticles join neighboring granules at the junction. This makes us expect that the electron transport through the bridge is bottlenecked at the junctions. Hence, experimentally studied resistance of the network is expected to be the series resistance of the granule-granule junctions.

The number of radical wires chemisorbed on a gold nanoparticle in the network was estimated to be ca. 17 on the basis of the elemental analysis. The ratio of the radical wires and gold nanoparticle was also evaluated to be ca. 15 independently from the magnetic susceptibility data measured by a SQUID magnetometer. This means at least 30 wires and the same number of *n*-hexanethiol molecules are coated on one nanoparticle because the wire molecules are shared by two nanoparticles. A spinless network was prepared similarly using SLM, and formation of a similar network structure was confirmed. The amount of spins in a gold nanoparticle of the spinless network is negligibly small on the basis of the magnetic susceptibility data.²¹

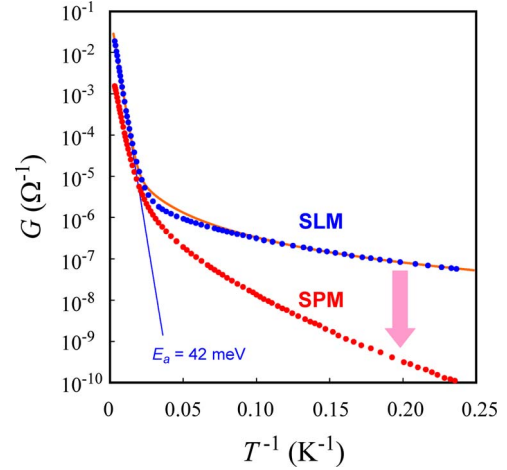


FIG. 3. (Color online) Conductance G of the SLM network (blue dots) and that of the SPM network (red dots) against the inverse temperature. The blue straight line shows the activation-type dependence with $E_a=42$ meV. The orange solid curve represents theoretical values predicted by Eq. (3).

B. Temperature dependence

In the present experiments, we note first that the charging energy of a nanoparticle at the junction, $E_{c_j}/k_B \approx 1800$ K ≈ 160 meV (vide ante), well exceeds the thermal energy (26 meV) at 300 K. Second, the tunnel resistance of a single terthiophenedithiol molecule (R_{ml}), which corresponds to the wire part of SPMs and SLMs, is roughly estimated to be as high as 10–100 M Ω through single molecule measurements.²⁷ Since neighboring nanoparticles are connected with ca. 30 wire molecules, the nanoparticle-nanoparticle tunnel resistance may be expected to be at least 0.3 M Ω –3 M Ω , which is well beyond the resistance quantum ($h/2e^2 \approx 13$ k Ω). Third, the voltage across each junction in the experiments, $V_j=V/N_j \approx 3$ mV ($V=0.1$ V and $N_j=30$), is well below $E_c/e \approx 160$ mV. Based on the three conditions above, the transport of the networks is supposed to be strongly influenced by the effect of Coulomb blockade due to gold nanoparticles.

Figure 3 plots $\log_{10}(G)$ vs T^{-1} for typical samples of both SLM and SPM networks. We find that in both networks the conductance is described by a thermal-activation-type behavior in a temperature range of 300 K–30 K,

$$G = \frac{1}{2R_t} \exp\left(-\frac{E_a}{k_B T}\right), \quad (1)$$

with $E_a=42$ meV for SLM network and $E_a=35$ meV for SPM network. In the lower T range (<30 K), the temperature dependence becomes distinctly weaker, where G_{SPM} is substantially smaller than G_{SLM} . Particularly, the T -dependence in the SLM network is approximated by $G \propto T^2$.

The ES-VRH law, $G \propto \exp\{-(T_0/T)^{1/2}\}$, is widely known in granular metals/semiconductors as well as in gold nanoparticle multilayers and thick films.^{14,15,28,29} The temperature dependence found here (Fig. 3) does not fit well with the ES-VRH law, but is interpreted as in the following.³⁰

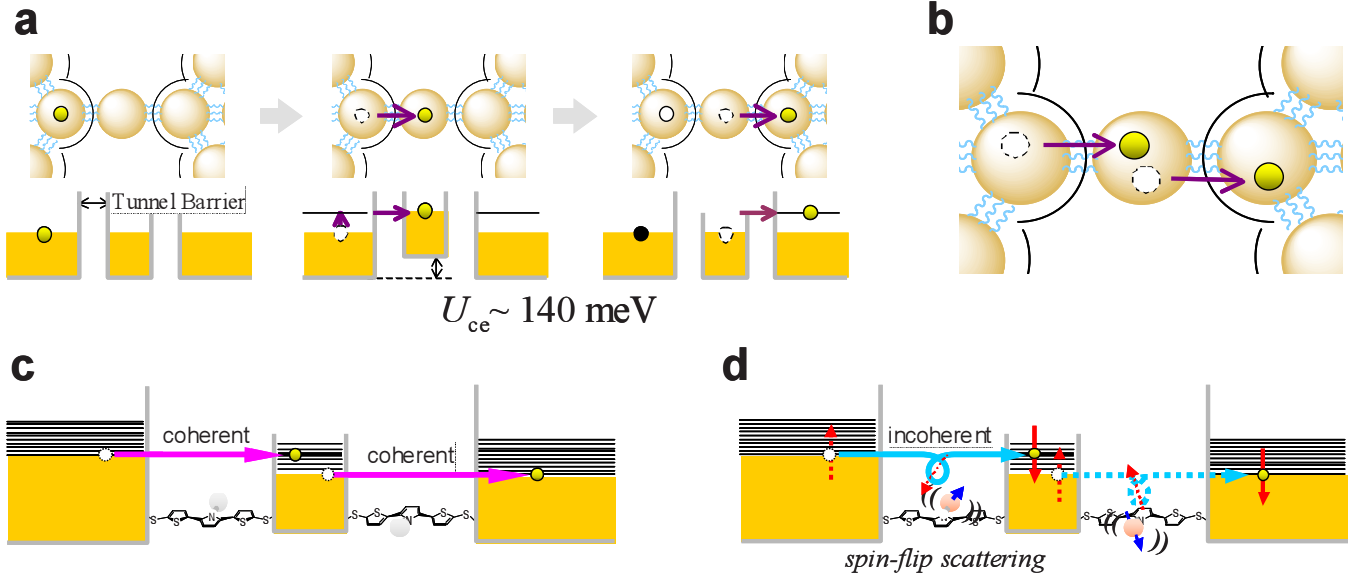


FIG. 4. (Color online) Schematic representation of electron transport in the networked gold nanoparticles. (a) T -assisted single electron tunneling and (b) Inelastic cotunneling across a Coulomb-blocked nanoparticle at an intergranule junction. (c) Cotunneling across the nanoparticle of the SLM network. (d) Spin-flip scattering of tunnel electrons by a local spin in the SPM network.

We start with the activation-type behavior seen at elevated temperatures. The activation energies ($E_a=42$ meV and 35 meV) are much smaller than the excitation energy between frontier orbitals of wire molecules (SOMO-LUMO or HOMO-LUMO). Instead, they are related to the charging energy of gold nanoparticles.³¹ The capacitance between a pair of nearest-neighbor nanoparticles is given by,³²

$$C_{\text{pair}} = 4\pi\epsilon_0\epsilon_r \frac{1 - r^2/d^2}{2/r - 2/d} \approx 5.0 \times 10^{-19} \text{ F}, \quad (2)$$

where $\epsilon_r \approx 2$ is the relative permittivity of the medium surrounding nanoparticles,³³ ϵ_0 is the dielectric constant of vacuum, $r=2.0$ nm is the particle radius, and $d=1.6$ nm is the intersurface gap distance between particles. We assume that the number of nearest-neighbor nanoparticles for a gold nanoparticle at a granule-granule junction is $n \approx 2$ [Fig. 2(b)]. The relevant capacitance may be approximated by $C \approx nC_{\text{pair}} \approx 1 \times 10^{-18}$ F, which yields a charging energy of $E_{c_j} = e^2/C \approx 160$ meV. The activation energy of a particular junction may take a value in the range of $0 < E_a < E_{c_j}/2$, where a particular value is determined by the local electrostatic potential at the junction. The local potential may be randomly distributed among relevant junctions. We hence suppose, for simplicity, that the experimentally found activation energy should be the average, $E_a \approx E_c/4 \approx 40$ meV. This value is close to the experimentally found values ($E_a = 35$ meV and 42 meV). The analysis above thus supports the interpretation that the resistance is determined by granule-granule junctions, through which conductance occurs via thermal activation of Coulomb-blocked gold nanoparticles.

We also mention that (i) inside granules a number of parallel junctions are available for electron conduction and (ii) E_c of nanoparticles inside granules should be substantially smaller than $E_{c_j} \approx 160$ meV because the number of neigh-

boring nanoparticles should be much larger than $n=2$: If one assumes hcp packing with $n=12$, $E_{c_g} \approx 27$ meV. These two facts make it highly probable that the conduction is bottlenecked at the granule-granule junctions.

At temperatures lower than 30 K, the conductance is much larger than the values expected from the thermal activation law [Eq. (1)]. We suggest as a relevant mechanism inelastic cotunneling process,²⁰ in which electrons simultaneously tunnel through more than one junction without paying the cost of charging energy [Fig. 4(b)]. The contribution of the cotunneling process, in the case when the number of relevant junction is $N=2$, is represented by the second term in the equation below:²⁰

$$G = \frac{1}{2R_t} \exp\left(-\frac{E_a}{k_B T}\right) + \frac{h}{6\pi^2 e^2 R_t^2 E_a^2} [(2\pi k_B T)^2 + (eV)^2]. \quad (3)$$

With $V=3$ mV, the T^2 -term dominates the V^2 -term down to $T=6$ K, and accounts for the T^2 -dependence found in the SLM network in a range of lower T .

Theoretically, the cotunneling conductance has to be consistent with the thermal-activation-type conductance by sharing two common parameters, R_t and E_a , as shown in Eq. (3). Hence we can check the consistency of our interpretation by fitting the data in the entire T -range to Eq. (3). Since $E_a = 42$ meV has been fixed, R_t is the only adjustable parameter. The experimental data of the SLM network is surprisingly well reproduced by Eq. (3) in the entire range of T as shown by the solid orange line in Fig. 3 if $R_t=3.6$ M Ω is assumed. As discussed in the beginning of this section, the number of wire molecules surrounding one nanoparticle was evaluated to be 30. If the closed packing model of nanoparticles in the network is assumed, the coordination number is 12. Hence the number of wire molecules connecting two

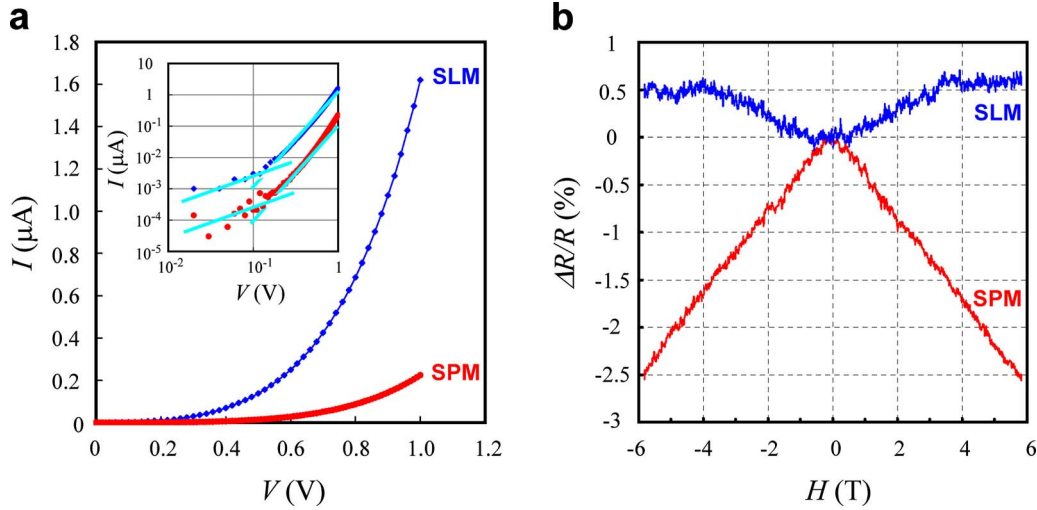


FIG. 5. (Color online) (a) Current-voltage characteristics in SLM and SPM networks ($T=4.2$ K). The inset displays log-log plots. (b) Magnetoresistance of SPM and SLM networks at 4.2 K (1 V). The SPM network exhibits negative magnetoresistance, while the SLM network shows a weakly positive magnetoresistance.

adjacent nanoparticles is evaluated to be ca. 3. When the tunnel resistance between a pair of nanoparticles (R_t) is multiplied by the number of connecting molecules, the molecular tunnel resistance of the wire molecule (R_{mt}) could be evaluated to be ca. 11 M Ω . Since the reported value of the tunnel resistance of terthiophenedithiol was 10–100 M Ω (Ref. 27), R_{mt} evaluated above may not be unreasonable for the SLM wire molecule. It is worthwhile to mention that the tunneling resistance of π -wire molecules ($R_{mt}=\text{ca. } 10$ M Ω) is smaller than that of σ -type wire molecules ($R_{mt}=\text{ca. } 2$ G Ω) by two orders of magnitude.³⁴ The utilization of a π -conjugated wire molecule with a higher probability of tunneling also contributes to raise the temperature at which cotunneling effect becomes evident (vide infra).³⁵

C. I - V characteristics

Additional evidence for cotunneling is obtained from the I - V characteristics studied at 4.2 K. As shown in Fig. 5(a), the current increases superlinearly as $I \propto V^3$ in both SLM and SPM networks when V exceeds 0.1 V ($3 \text{ meV} < eV/N_J$). This can be attributed to the V^2 term in Eq. (3), which dominates when $2\pi k_B T < eV_J$. The nonlinearity occurs in a region of $eV/N_J < E_c$, which rules out the well-known feature of the “Coulomb staircase.”¹¹ Equation (3) considers a single Coulomb island connected through two tunnel junctions to reservoirs.²⁰ According to generalized theories of cotunneling, the higher-order power law, $I \propto V^{2N-1}$, is expected when cotunneling occurs in N junctions.³² Our analysis therefore strongly suggests that $N=2$ in our experiments, which is consistent with the assumption that the resistance we measure is determined by the granule-granule junctions [Fig. 2(b)].

As mentioned in Sec. III B, the T -dependence in the present experiments is not well reproduced by the ES-VRH law, which has been reported widely in recent experiments on nanoparticle networks.^{14,28,29} Recently, theoretical approaches have been developed based on *multiple cotunneling* in disordered systems, and the ES-VRH law has been

derived.^{36–39} Higher-order power law in the I - V characteristic ($N \gg 2$) was found in multilayer films of thiol-derivatized gold nanoparticles without wire molecules, and the results were discussed in terms of the *multiple cotunneling* based ES-VRH model.^{15,40,41} As to the difference of the present experiments from those studies, we suggest that the resistance studied here is the one of the granule-granule junction. The number of relevant gold nanoparticles is hence limited practically to unity, so that $N=2$. First, the possible path of cotunneling may be uniquely determined at a given granule-granule junction, making impossible the occurrence of ES-VRH-type behavior. Second, in the case of $N=2$ the distance over which an electron effectively moves via cotunneling may be too small for deriving the ES-VRH-type conductance.

D. Influence of localized spin

In the lower- T range, the conductance of SPM network is distinctly smaller (Fig. 3) than that of SLM network and cannot be explained by Eq. (3). We found that this difference is systematic and reproducible. We hence suggest that the isolated spin on wire molecules disturbs cotunneling process in the SPM network [Fig. 4(d)]. When an electron tunnels from one nanoparticle to another through a SPM wire, the electron may undergo spin-flip scattering due to the exchange interaction with localized spin on the wire molecule. We note that the theory of cotunneling implicitly assumes that individual tunneling events at respective junctions are elastic-and-nonmagnetic processes (without spin-flip scattering):^{40,41} For this, whether the cotunneling is elastic or inelastic is irrelevant. We expect therefore that the probability of cotunneling is substantially reduced if the individual tunneling is of a spin-flip character.

We found that the conductance of the SPM network increases with increasing magnetic field as shown by the red line in Fig. 5(b), where the resistance at 4.2 K is displayed as a function of magnetic field up to ± 6 T. (The bias voltage is

fixed at $V=0.1$ V. The rate of magnetic field sweep is $0.5 \text{ T}\cdot\text{min}^{-1}$.) The negative magnetoresistance, $[R(6 \text{ T}) - R(0 \text{ T})]/R(0 \text{ T})$, amounts to -2.5% at $B=6 \text{ T}$.^{16,42} On the other hand, slightly positive magnetoresistance which was plotted in blue, was detected in the SLM network. As reference measurements, we scavenged the localized spin in the SPM network by treating with hexanethiol. Though not shown in Fig. 5(b), the negative magnetoresistance was found to vanish after this treatment.

Since magnetic fields define the preferable orientation for localized spins, the spin-flip scattering is suppressed by the magnetic fields, and the probability of cotunneling is recovered. Thus the negative magnetoresistance in the SPM network provides unequivocal evidence that the spin-flip scattering is attributed to the localized spin on the wire molecule. This is the first experimental demonstration that the organic localized spin can interact with itinerant electrons which tunnel through the wire molecule.⁴² This scheme is distinguished from the conventional scheme of quantum-dot spintronics, which aims at manipulating the electron spin state in the quantum dot.^{4,5}

It is to be noted that the resistance of the SPM network linearly depends on the magnetic field [Fig. 5(b)]. This may be ascribed to an extremely low density of states, basically arising solely from a single SOMO of the wire molecule. The linear magnetic-field dependence is in contrast to the bell-shaped trace of ferromagnetic metals, the magnetization curve of which exhibits easy saturation.

IV. CONCLUSION

We constructed network structures by connecting gold nanoparticles with spin-polarized and spinless wire mol-

ecules. It was found that these networks exhibited a thermal-activation-type conduction in a higher temperature range, $300 \text{ K} > T > 30 \text{ K}$, and that its temperature dependence becomes much weaker at temperatures lower than 30 K . The characteristic behavior is interpreted in terms of the thermally activated tunneling between nanoparticles and the cotunneling between plural nanoparticles, respectively. Judging from the temperature dependence of the conductance and from the I - V characteristics of the networks, the above findings originated from the large charging energy of the nanoparticle that worked as a Coulomb island. It was revealed that the decrease in the conductance of the spin-polarized network in the low-temperature region was much larger than that of the spinless network. Moreover, the spin-polarized network exhibited negative magnetoresistance upon application of the external magnetic field. These results were unequivocally rationalized by the interaction between localized spin in a π -orbital of the organic radical and the tunneling single electron through the molecular wire connecting metallic nanoparticles. This discovery that the localized spin which exists in the tunnel barrier perturbs the cotunneling on the basis of the spin-flip mechanism is substantial in the development of molecule-based spinoelectronics. In the future, a spintronic device with a processing or a memory-storage function could be developed by switching on or off a spin on the wire molecule in terms of redox and photo-responsive abilities.

ACKNOWLEDGMENTS

This work was supported by a Grant-in-Aid for Scientific Research on Priority Areas "Application of Molecular Spins" (Area No. 769, Proposal No. 15087101) from the Ministry of Education, Culture, Sports Science and Technology (MEXT).

*suga@pentacle.c.u-tokyo.ac.jp

†skomiyama@thz.c.u-tokyo.ac.jp

¹G. A. Prinz, *Science* **282**, 1660 (1998).

²M. Johnson, *J. Phys. Chem. B* **109**, 14278 (2005).

³R. Fiederling, M. Keim, G. Reuscher, W. Ossau, G. Schmidt, A. Waag, and L. W. Molenkamp, *Nature (London)* **402**, 787 (1999).

⁴K. Tsukagoshi, B. W. Alphenaar, and H. Ago, *Nature (London)* **401**, 572 (1999).

⁵K. Ono, D. G. Austing, Y. Tokura, and S. Tarucha, *Science* **297**, 1313 (2002).

⁶C. Joachim, J. K. Gimzewski, and A. Aviram, *Nature (London)* **408**, 541 (2000).

⁷J. Nakazaki, I.-G. Chung, M. M. Matsushita, T. Sugawara, R. Watanabe, A. Izuoka, and Y. Kawada, *J. Mater. Chem.* **13**, 1011 (2003).

⁸J. Nakazaki, I.-G. Chung, R. Watanabe, T. Ishitsuka, Y. Kawada, M. M. Matsushita, and T. Sugawara, *Internet Electron. J. Mol. Des.* **2**, 112 (2003).

⁹H. Sakurai, A. Izuoka, and T. Sugawara, *J. Am. Chem. Soc.* **122**, 9723 (2000).

¹⁰M. M. Matsushita, H. Kawakami, Y. Kawada, and T. Sugawara,

Chem. Lett. **36**, 110 (2007).

¹¹M. Brust, M. Walker, D. Bethell, D. J. Schiffrin, and R. Whyman, *J. Chem. Soc., Chem. Commun.* **1994**, 801.

¹²R. S. Ingram, M. J. Hostetler, R. W. Murray, T. G. Schaaff, J. T. Khoury, R. L. Whetten, T. P. Bigioni, D. K. Guthrie, and P. N. First, *J. Am. Chem. Soc.* **119**, 9279 (1997).

¹³G. Schmid, *Chem. Rev. (Washington, D.C.)* **92**, 1709 (1992).

¹⁴T. B. Tran, I. S. Beloborodov, X. M. Lin, T. P. Bigioni, V. M. Vinokur, and H. M. Jaeger, *Phys. Rev. Lett.* **95**, 076806 (2005).

¹⁵P. Sheng, in *Nanophase Materials*, edited by G. C. Hadjipanayis and R. W. Siegel (Kluwer, Dordrecht, 1994), p. 381.

¹⁶Negative magnetoresistance due to weak localization effect has been reported by J. L. Dunford, A.-A. Dhirani, and B. W. Statt, *Phys. Rev. B* **74**, 115417 (2006) on a gold nanoparticle network connected with butanedithiol. The amplitude, however, is much smaller.

¹⁷T. Ogawa, K. Kobayashi, G. Masuda, T. Takase, and S. Maeda, *Thin Solid Films* **393**, 374 (2001).

¹⁸S. Taniguchi, M. Minamoto, M. M. Matsushita, T. Sugawara, Y. Kawada, and D. Bethell, *J. Mater. Chem.* **16**, 3459 (2006).

¹⁹M. Minamoto, M. M. Matsushita, and T. Sugawara, *Polyhedron* **24**, 2263 (2005).

- ²⁰D. V. Averin and Y. V. Nazarov, in *Single Charge Tunneling: Coulomb Blockade Phenomena in Nanostructures*, edited by H. Grabert and M. H. Devoret (Plenum/NATO Scientific Affairs Division, New York, 1992), p. 217.
- ²¹Y. Negishi, H. Tsunoyama, M. Suzuki, N. Kawamura, M. M. Matsushita, K. Maruyama, T. Sugawara, T. Yokoyama, and T. Tsukuda, *J. Am. Chem. Soc.* **128**, 12034 (2006).
- ²²D. Jones, M. Guerra, L. Favaretto, A. Modelli, M. Fabrizio, and G. Distefano, *J. Phys. Chem.* **94**, 5761 (1990).
- ²³J. L. Brédas, R. Silbey, D. S. Boudreaux, and R. R. Chance, *J. Am. Chem. Soc.* **105**, 6555 (1983).
- ²⁴W. M. H. Sachtler, G. J. H. Dorgelo, and A. A. Holscher, *Surf. Sci.* **5**, 221 (1966).
- ²⁵T. Tada and K. Yoshizawa, *ChemPhysChem* **3**, 1035 (2002).
- ²⁶M. M. Maye, S. C. Chun, L. Han, D. Rabinovich, and C.-J. Zhong, *J. Am. Chem. Soc.* **124**, 4958 (2002).
- ²⁷C. Kergueris, J.-P. Bourgoin, S. Palacin, D. Esteve, C. Urbina, M. Magoga, and C. Joachim, *Phys. Rev. B* **59**, 12505 (1999).
- ²⁸H. E. Romero and M. Drndic, *Phys. Rev. Lett.* **95**, 156801 (2005).
- ²⁹D. Yu, C. Wang, B. L. Wehrenberg, and P. Guyot-Sionnest, *Phys. Rev. Lett.* **92**, 216802 (2004).
- ³⁰The experimental plots deviate from the conventional ES-VRH model if the hopping distance varies depending on the temperature even in the ES-VRH regime: J. L. Dunford, Y. Suganuma, A. A. Dhirani, and B. Statt, *Phys. Rev. B* **72**, 075441 (2005).
- ³¹L. P. Kouwenhoven, G. Schön, and L. L. Sohn, in *Introduction to Mesoscopic Electron Transport*, edited by L. L. Sohn, L. P. Kouwenhoven, and G. Schön (Kluwer, Dordrecht, 1997), pp. 1–44.
- ³²H. Stöcker, *Taschenbuch Der Physik (Handbook of Physics)* (Verlag Harry Deutsch, Frankfurt am Main, 1998).
- ³³The relative permittivity of π -conjugated wire molecules and surfactants is nearly 4. Although the nanoparticles are densely covered with the molecules and surfactants, the surrounding medium cannot be assumed to be of the most closely packed structure. We hence assume that the relative permittivity of surroundings of a nanoparticle is about 2.
- ³⁴J. He, F. Chen, J. Li, O. F. Sankey, Y. Terazono, C. Herrero, D. Gust, T. A. Moore, A. L. Moore, and S. M. Lindsay, *J. Am. Chem. Soc.* **127**, 1384 (2005).
- ³⁵Energy levels in gold nanoparticles are discrete due to size-quantization with a separation roughly estimated to be $\Delta E \approx (2/3)(E_F/N_e) \approx 2.1$ meV, where $E_F=5.5$ eV is the Fermi energy and $N_e \approx 1750$ is the number of conduction electrons in a nanoparticle. Because $\Delta E \approx 2.1$ meV $< eV_j \approx 3$ meV ($\ll E_c/e \approx 160$ mV), the discreteness may not substantially affect our discussion.
- ³⁶M. V. Feigel'man and A. S. Ioselevich, *JETP Lett.* **81**, 277 (2005).
- ³⁷I. S. Beloborodov, K. B. Efetov, A. V. Lopatin, and V. M. Vinokur, *Phys. Rev. Lett.* **91**, 246801 (2003).
- ³⁸I. S. Beloborodov, A. V. Lopatin, and V. M. Vinokur, *Phys. Rev. B* **72**, 125121 (2005).
- ³⁹I. S. Beloborodov, A. Glatz, and V. M. Vinokur, *Phys. Rev. B* **75**, 052302 (2007).
- ⁴⁰D. V. Averin and Yu. V. Nazarov, *Phys. Rev. Lett.* **65**, 2446 (1990).
- ⁴¹L. J. Geerligs, D. V. Averin, and J. E. Mooij, *Phys. Rev. Lett.* **65**, 3037 (1990).
- ⁴²Spin-flip scattering in magnetic junction with paramagnetic impurity was discussed and a higher resistance and lower magnetoresistance were expected as results of the spin-flip scattering on the paramagnetic impurity. See F. Guinea, *Phys. Rev. B* **58**, 9212 (1998).